

Organic Electro-Optic Materials: Some Unique Opportunities

L. R. Dalton^a, A. K. Y. Jen^{a,b}, W. H. Steier^c, B. H. Robinson^a, S. H. Jang^a, O. Clot^a, H. C. Song^c, Y. H. Kuo^c, C. Zhang^c, P. Rabiei^c, S. W. Ahn^c, and M. C. Oh^c

Departments of ^aChemistry and ^bMaterials Science & Engineering, University of Washington, Seattle, WA 98195

^cDepartment of Electrical Engineering, University of Southern California, Los Angeles, CA 90089

ABSTRACT

Recent use of quantum mechanics to guide the improvement of molecular hyperpolarizability and the use of statistical mechanical analysis of the effects of intermolecular electrostatic interactions to improve the acentric ordering of organic chromophores has led to the realization of electro-optic coefficients, r_{33} , greater than 100 pm/V (at telecommunication wavelengths). This material design and development paradigm is likely to lead to further improvement in electro-optic activity, which will in turn facilitate the development of a variety of electro-optic devices with drive (V_{π}) voltage requirements of less than one volt. The utility of organic electro-optic materials for development of high bandwidth devices is now well documented. What is less obvious is the utility of organic electro-optic materials for the fabrication of complex (including conformal, flexible, and three-dimensional) device structures. In this communication, we review recent improvements in electro-optic activity; thermal and photochemical stability; and processability of organic electro-optic materials and the use of these materials to fabricate conformal and flexible electro-optic devices and devices based upon single and multiple coupled ring microresonators.

Keywords: Electro-optic materials and devices, hyperpolarizability, ring microresonators, WDM

1. INTRODUCTION

The advantages of organic electro-optic materials for the fabrication of high bandwidth devices have been known for some time.¹⁻⁸ Also, the potential for systematically improving molecular hyperpolarizability and hence electro-optic activity through the use of quantum mechanical guidance has been appreciated for more than two decades.⁵⁻¹⁵ The dependence of molecular first hyperpolarizability, β , on length of the chromophore's π -electron system, the symmetry of the π -electron system, and bond-length alternation has been investigated for more than a decade. More recently, attention has focused on defining the effect of substituents on molecular hyperpolarizability⁸ although the reader's attention is also called to an article in this issue dealing with the theoretical examination of multiple donor/acceptor chromophores.¹⁶ Focus on defining the effect of altering substituents to a basic core chromophore structure is a very productive paradigm for the practical improvement of molecular hyperpolarizability because the insight gained is easily transitioned to organic chemists for synthesis of improved chromophores--that is, synthesis of a new and improved chromophore can frequently be accomplished by modification of one or only a few steps of a multiple step synthesis of the complete chromophore.⁸ Moreover, quantum mechanical predictions are frequently more reliable when comparing variations among structurally similar chromophores. Factors such as changing molecular conformation can make predictions as a function of length more difficult and predictions related to bond length alternation can be compromised by steric effects that influence the dihedral angle relating π -orbitals. A relatively minor structure modification (for example, the replacement of a single cyano group of a tricyanofuranvinylene acceptor (see Fig. 1) with a nitro group) can lead to significant improvement in molecular hyperpolarizability with little or no impact on chromophore conformation.⁸ In the next section (Theory), we review recent successes that we have had with modification of chromophore acceptor structure and in particular replacement of the tricyanofuranvinylene acceptor with a tricyanopyrrolinevinylene acceptor. We also suggest other structures that should lead to still larger increases in molecular hyperpolarizability. In addition to calculation of molecular hyperpolarizability, β , calculations of dipole moment, μ , is of interest and an excellent comparison of different computational methods has recently been published.¹⁷

The principle component of the electro-optic tensor, r_{33} , for dipolar electro-optic polymers can be related to molecular hyperpolarizability through the following expression:

$$r_{33} = N \langle \cos^3 \theta \rangle > 2F\beta/n^4 \quad (1)$$

where N is the chromophores number density, $\langle \cos^3 \theta \rangle$ is the acentric (noncentrosymmetric) order parameter, F is the local field factor taking into account the dielectric nature of the host environment, and n is the index of refraction. In the absence of intermolecular electrostatic interactions, $\langle \cos^3 \theta \rangle = \mu F E_p / 5kT$ where μ is the chromophore dipole moment, E_p is electric poling field strength, and kT is the thermal energy. In the presence of intermolecular electrostatic interactions, W , the expression for order parameter must be modified to include an attenuation factor, $[1 - L^2(W/kT)]$:

$$\langle \cos^3 \theta \rangle = (\mu F E_p / 5kT) [1 - L^2(W/kT)] \quad (2)$$

where L is the Langevin function.¹⁸⁻²¹ Since W depends on N , the order parameter is observed to independent of chromophore concentration at low concentration but is predicted to decrease to zero as concentration is increased. Thus, electro-optic activity is predicted to initially increase linearly with N (and with μ) but then is predicted to go through a maximum and decrease with increasing concentration at high N . The position of the maximum of a plot of r_{33} versus N is approximately given by $N_{\max} = 1.38T/\mu^2$. Eqn. (2) is an over-simplification in that nuclear repulsive (steric interactions) have been neglected. We have shown how these are straightforwardly taken into account (including within a hard object approximation).^{20,21} Since nuclear repulsive interactions are short ranged, their effect will be noticed at high concentrations and the primary effect is to make the plots of r_{33} versus N appear more symmetrical.

With the above remarks in mind, it is clear that optimization of electro-optic activity is a matter of optimizing $N \langle \cos^3 \theta \rangle$ for a given chromophore (i.e., a given β). Because μ is frequently observed to increase with increases in β , it is difficult to achieve translation of more than a few percent of the effective molecular electro-optic activity of a chromophore to macroscopic electro-optic activity when the dipole moment of the chromophore exceeds 10 Debye. Recently, we have identified several schemes for increasing β without increasing μ ; one such scheme is discussed elsewhere in this volume.¹⁶ However, as noted elsewhere,^{22,23} consideration of the competition of electronic and nuclear (steric) interactions suggests a very straightforward paradigm for improving the maximum achievable electro-optic activity that can be realized for a given π -electron structure. Electronic properties will be dominated by π -electrons and thus intermolecular electronic electrostatic interactions will be defined by the component of the chromophore structure containing π -orbitals. The electronic electrostatic potential felt by a reference chromophore from surrounding chromophores will consist of two parts--one favoring centrosymmetric ordering of chromophores and the other favoring desired noncentrosymmetric (acentric) ordering.¹⁹⁻²¹ The relative magnitudes of these two contributions can be tuned by adjusting the spatially anisotropic nuclear repulsive potential (i.e., by changing the shape of the chromophore without changing the π -electron structure).¹⁸⁻²³ This can be accomplished by attaching saturated substituents (e.g., alkyl groups) to the π -electron backbone. Unsaturated substituents can also be used providing the π -electron conjugation of the substituents is sufficiently short to avoid contributing to μ and β . Considering overall chromophore shape, the worst possible shape is a prolate ellipsoidal shape that permits close side-by-side approach of chromophores. Such an approach strongly favors centrosymmetric ordering and explains the common observation of centrosymmetric crystal structures for rod-like, high dipole moment chromophores. Electro-optic activity can be improved by making chromophores more spherical in overall shape.²⁰⁻²³ In the next section, we present another experimental example of this phenomenon.

The above analysis is appropriate for consideration of chromophores physically dissolved in host polymers to produce composite materials or covalently attached by a single bond to polymer backbone such that the chromophore can move independently of the polymer host during electric field poling. Indeed, the simple theory presented above has both explained experimentally observed data and permitted estimation of the maximum electro-optic activity that can be achieved for a given chromophore structure (and the chromophore number density, N , that led to the maximum value). If covalent attachment of the chromophore to the polymer or dendrimer host material significantly restricts the movement of chromophores under the action of a poling field, then a theoretical analysis that takes these additional interaction potentials into account must be employed. This will typically involve use of a variant of atomistic Monte Carlo computation methods.^{19,24} Robinson and coworkers have suggested a computationally efficient pseudo-atomistic Monte Carlo approach that treats sections of the overall structure that contain conjugated π -electrons as rigid objects while treating flexible segments in a fully atomistic manner.²⁵ Since π -conjugation restricts rotation about bonds, this is a reasonable approximation. This approach helps understand the folding of multi-chromophore-containing dendrimers^{23,26} under electric field poling and helps to understand why various chromophores can form H and J

aggregate structures. In addition to understanding electrically poled materials, this pseudo-atomistic Monte Carlo approach is appropriate for understanding the electro-optic activity observed for high dipole moment chromophore ordered by sequential synthesis or self-assembly methods.²⁷⁻²⁹ The additional consideration of the effect of covalent bond restrictions naturally leads to a number of other design paradigms for improving macroscopic electro-optic activity including the use of dendronized polymer materials.^{23,30,31} Such materials have led to factors of two improvement in electro-optic activity relative to the best value that can be obtained for the same chromophore in composite materials.²³ Pseudo-atomistic Monte Carlo calculations suggest a variety of structures that lead to improved electro-optic activity and may guide the systematic design of perfect noncentrosymmetric (ferroelectric) order for some organic materials.

The adoption of a more global strategy for the engineering of optimized electro-optic activity has the advantage of permitting auxiliary properties such as optical loss, conductivity, index of refraction, etc. to be simultaneously optimized. For example, the use of partially fluorinated dendrimers incorporating electro-optic chromophores has permitted the realization of organic waveguide materials exhibiting optical loss values of less than 1 dB/cm and values as low as 0.2 dB/cm at 1.55 microns telecommunications wavelengths.^{7,30-35} It has permitted a variety of options for lattice hardening (intra and intermolecular crosslinking) to be pursued and affords promise for improved thermal stability. New crosslinking chemistries that do not involve the elimination of water have been developed and potentially viable photocrosslinking reactions are being investigated.^{7,30-35}

Synthetic efficiency is of concern as it translates to cost of production of materials and the ability to produce materials in kilogram quantities. A recent and general advance in this area has been the utilization of microwave-assisted synthesis techniques to improve reaction yields and reduce reaction times.³⁶ A number of more modest improvements in specific synthetic routes have also been achieved but are beyond the scope of this article.

The photostability of organic materials remains an issue of concern. Reactions involving singlet oxygen are of concern for all organic chromophores and recently Stegeman and coworkers³⁷ have shown that a second class of photo-induced reactions can be important for chromophores capable of trans-cis isomerization (stilbenes and azobenzenes). Photodegradation involving oxygen can be attenuated by exclusion of oxygen (including by appropriate packaging), by use of physical and chemical quenching of singlet oxygen, by lattice hardening to limit oxygen diffusion, and by steric protection or elimination of sites prone to singlet oxygen attack. While much additional study of photostability in specific organic electro-optic materials is required, it appears likely that acceptable stability can be achieved for current telecommunication power levels.

Stability under the presence of space radiation (gamma rays and high energy particles) appears to be more promising although more research and more publication of results collected in various laboratories needs to be forthcoming. The π -electron system of organic electro-optic materials may help attenuate radiation-induced damage by quickly relaxing charge perturbations produced by the high-energy particles and rays. Early studies certainly suggest exceptional stability for organic electro-optic materials.

A distinct advantage of organic electro-optic materials is their processability. Thin films can be prepared by spin coating and by a variety of deposition methods. Active and passive waveguide circuitry can be fabricated in these films by standard reaction ion etching or photochemical processing.^{6,7} By use of special masking techniques, vertical transitions can be fabricated relevant to the production of low insertion loss electro-optic structures and three-dimensional circuits.^{6,7,38-40} Electro-optic circuitry can be fabricated directly on top of semiconductor VLSI circuitry with preservation of the performance of both types of circuitry. A wide variety of device structures ranging from stripline,^{6,7,41-48} to cascaded prism,^{6,7,49-51} to ring microresonators^{23,52,53} (and photonics bandgap) have been fabricated. Moreover, organic electro-optic devices can be fabricated so as to be conformal or flexible; for example, as relevant to the production of phased array radar including space deployable antennae structures.⁵⁴ In the following section on devices, we demonstrate the little appreciated fact that organic electro-optic devices (like organic light emitting devices) can be conformal and flexible. We will also illustrate the utility of organic electro-optic materials for the fabrication of ring microresonator devices.

2. THEORY

2.1. Quantum mechanical calculations of molecular hyperpolarizability

As noted above, the use of quantum mechanics to predict the variation of molecular hyperpolarizability with simple modification of molecular structure has proven to be quite effective. We illustrate this point in Fig. 1 showing semi-empirical calculation of β , μ , and λ_{\max} for two chromophores that differ only in the acceptor portion of the molecule.

The results shown here suggest that replacement of the furan group of the tricyanofuranvinylene acceptor with a pyrroline group should lead to a significant improvement in molecular hyperpolarizability with little or no effect on

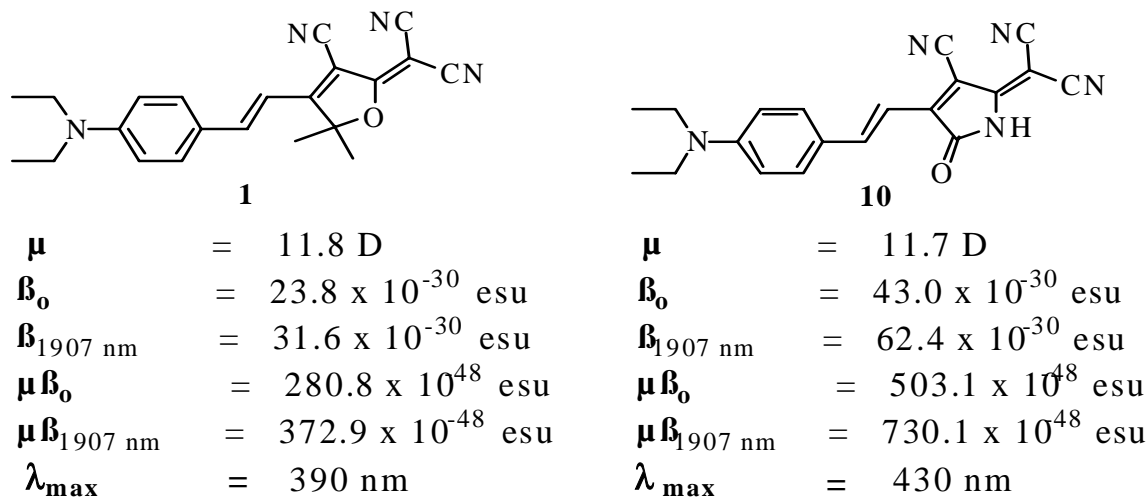


Figure 1. Semi-empirical calculations of dipole moment (μ), molecular hyperpolarizability (β) and absorption maximum of the HOMO-LUMO (charge transfer) transition are shown for two chromophore structures.

dipole moment. This should in turn translate to an improvement in macroscopic electro-optic activity given the similarity of the dipole moments and molecular structures. Preliminary Hyper Rayleigh scattering measurements suggest that this theoretically-predicted trend is correct although more measurements are needed before this conclusion can be put forward with confidence. However, use of this new acceptor with an amine donor and a phenylvinylene-thiophenevinylene bridge led to a measured electro-optic coefficient, r_{33} , of 101 pm/V at 1.55 microns for 20 % (by weight) loading of this chromophore in amorphous polycarbonate (APC, Aldrich). This is quite an exceptional value and certainly is approximately double the value typically obtained with chromophores containing the tricyanofuranvinylene acceptor. Exploiting the "gradient bridge" concept introduced by McMahan and coworkers¹³ would seem to suggest that an even more dramatic enhancement in hyperpolarizability can be achieved. Consider the following structure for which we show the results semi-empirical quantum mechanical calculations:

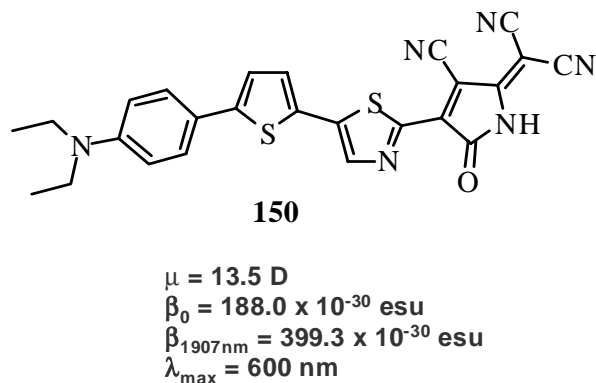


Figure 2. The results of semi-empirical quantum mechanical calculations are shown for a chromophore containing a thiophene-thiazole gradient bridge and a tricyanopyrrolinevinylene acceptor.

Gradient bridge structures are discussed in greater detail elsewhere in this volume. The theoretical suggestions evident from Fig. 2 have yet to be tested but we are presently synthesizing a number of variants of gradient bridge chromophores as well as chromophores containing new donors and acceptors that have been suggested by quantum

mechanical calculations to lead to improvement in molecular hyperpolarizability. What is very likely is that electro-optic coefficients on the order of 200 pm/V at telecommunication wavelengths will be achieved by the end of 2004 with values as high as 180 pm/V already being observed in preliminary characterization studies of newly synthesized chromophores. However, it should be clear to the reader that a great deal of characterization measurements will be required before paradigms for the systematic improvement of organic electro-optic chromophores can be clearly established. It should also be realized that it will likely be some time before ultimate hyperpolarizability will be achieved for "device-relevant" chromophores. By "device-relevant" chromophore we refer to chromophores possessing appropriate auxiliary properties as well as large molecular hyperpolarizability.

2.2. Statistical mechanical calculations of chromophore order

As noted above, two straightforward approaches exist for improving $N\langle\cos^3\theta\rangle$ and thus macroscopic electro-optic activity. The first is to modify simple chromophore structures to make them more spherical. Recent theoretical calculations suggest that a 2 to 1 length to width aspect ratio would represent both a significant improvement in $N\langle\cos^3\theta\rangle_{\max}$ and may be an achievable target. Recently, we have modified tricyanofuranvinylene acceptor containing chromophores with ProDOT-modified dithiophene bridges (see Fig. 3) and have measured electro-optic coefficients of 115 pm/V at 1.3 microns.

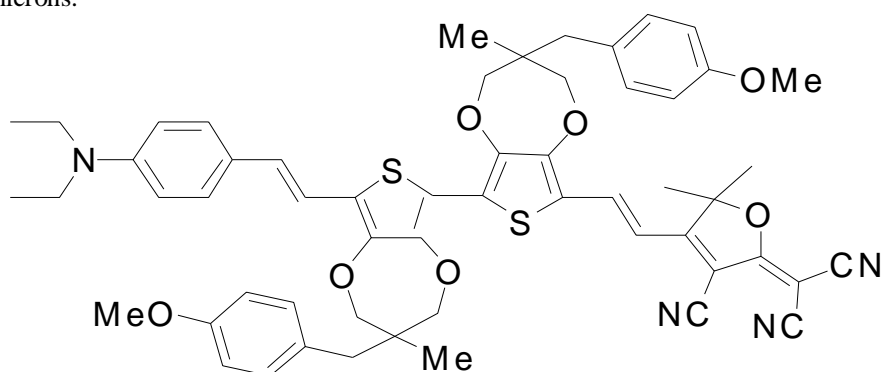


Figure 3. A ProDOT chromophore structure leading to an electro-optic coefficient of 115 pm/V at 1.3 microns for 30% loading of the chromophore in APC is shown. An electro-optic coefficient of 69 pm/V is observed at 20% loading.

While such chromophores may not achieve the desired aspect ratio, they are significant for providing a fundamental structure that can be further modified to more toward the desired goal. The ProDOT-modified dithiophene bridges are just one example of bridges offering structural control appropriate for improving $N\langle\cos^3\theta\rangle$. We initially focused on this structure because both the ProDOT structure and dithiophene bridges lead to improved molecular hyperpolarizability as well as providing an appropriate platform for aspect ratio modification. A number of characterization measurements will have to be carried out including independent measurements of molecular hyperpolarizability, dipole moment, electro-optic activity, photochemical stability, order parameter, etc.

It is interesting to note that the measured value of 115 pm/V may not be the maximum achievable electro-optic activity for this chromophore. We are currently carrying out measurements at 35 and 40% loading as well as filling in measurements at lower loading (15% and 25%). The observed significant increase in electro-optic activity in going from 20 to 30% loading attests to the fact that steric hindrance is working to produce a more favorable balance between intermolecular electrostatic forces that favor respectively acentric and centric order. However, considerably more experimental data will be required before this behavior can be modeled quantitatively. We are in the process of attempting to systematically collect such data.

While it is now clear from experimental data that incorporation of chromophores into dendronized polymers is an effective approach to improving electro-optic activity relative to that which can be achieved with guest-host composite materials, more detailed theoretical analysis of each specific example needs to be carried out to understand the importance of flexible components (for example, the length and positioning of flexible components). Although this is an area where we are starting to carry out a systematic correlation of theory and experiment, discussion of results will be deferred to a later publication.

The above two approaches to controlling intermolecular electrostatic interactions for the purpose of optimizing macroscopic electro-optic activity will likely lead to electro-optic coefficients on the order of 300 pm/V in the

reasonably near future. However, to achieve electro-optic coefficients on the order of 1000 pm/V, $N\langle\cos^3\theta\rangle$ will have to be enhanced to the point of approaching nearly perfect acentric (ferroelectric order).

Theory predicts that a way to achieve even greater electro-optic activity than achieved with simple chromophore derivatization or use of multi-chromophore-containing dendrimers and dendronized polymers is to synthesize multi-chromophore bundles where chromophores are held in an acentric arrangement in close proximity by strong covalent bonds. Several potential arrangements may lead to improved electro-optic activity: (1) Arrangements where 3 or 4 chromophores are covalently locked in a J aggregate configuration and (2) bundles that are composed of chromophores with both positive and negative molecular first hyperpolarizabilities. In this latter arrangement, dipole moments partially cancel while molecular first hyperpolarizability values add. We are currently synthesizing several such multi-chromophore bundles but characterization data are not yet available and detailed discussion of this approach must be deferred to a later publication. These arrangements have the advantage of being “minimum energy” configurations for the chromophores within the bundles. The remaining region around the bundle can be designed to minimize centrosymmetric organization of the bundles and to control solubility of the bundles. These bundles, like multi-chromophore-containing dendrimers and dendronized polymers eliminate the need for a host polymer. While it can be argued that the synthesis of supramolecular bundles, like the synthesis of low generation dendrimers, involves more effort than production of guest-host composite materials, these supramolecular structures permit systematic design of steric interactions that can also improve thermal and photostability and lead to materials exhibiting reduced optical loss.

It should be kept in mind that the same intermolecular electrostatic interactions that act to attenuate $N\langle\cos^3\theta\rangle$ for electrically poled polymer or dendrimer films also come into play in attenuating order for materials prepared by sequential synthesis or self-assembly methods. Chromophore design (“footprint”) is just as important for these approaches as it is for electric field poling. For example, intermolecular electronic (dipole-dipole, etc.) interactions will cause chromophores to tilt from the normal to the deposition surface when sequential synthesis approaches are used. This tilt will result in disorder that will increase as subsequent layers are deposited. However, when robotic methods are applied together with appropriate consideration of the shape of the chromophoric object to be deposited, exceptional values of electro-optic activity may be achieved with sequential synthesis/self assembly methods. These methods have the advantage (as in cases of crosslinked dendrimers, dendronized polymers, and supramolecular bundles) of having both ends of the chromophore attached to a crosslinked (and sterically-constrained) lattice. Such lattices exhibit dramatically improved thermal and photochemical stability relative to modest glass transition temperature chromophore/polymer composites. While new theoretically-inspired structures will likely lead to quite dramatically improved values of electro-optic activity and auxiliary properties, it will likely be several years before these materials can be fully evaluated and the limits of organic electro-optic activity defined.

3. DEVICES

3.1. Fabrication and characterization of conformal and flexible electro-optic modulators

A wide variety of stripline, prism (including cascaded prism and superprism), and resonated (ring microresonator and photonic crystal structures) devices have been fabricated from organic electro-optic materials. Organic materials have been fabricated on a variety of substrates including directly on top of (vertically integrated with) semiconductor VLSI wafers. This is straightforwardly accomplished by deposition of a “planarizing” polymer layer to achieve an optical quality deposition surface for subsequent spin casting of the active polymer layer. Three dimensional active circuit structures and low optical insertion loss structures have been fabricated using a variety of special masking techniques.

The most commonly investigated device structure has been stripline Mach Zehnder modulators. For these devices and using CLD/APC composite materials, drive voltages of 1.2 V (at 1.3 microns) and 1.8 V (at 1.55 microns) have been demonstrated for 2 cm length electrodes. The observed 3 dBe bandwidth was 18 GHz and found to be limited by rf metal loss of the electrodes. This latter observation is consistent with observations of Fetterman and coworkers and researchers at Lucent. Mach Zehnder devices fabricated using organic electro-optic materials on flexible substrates can be used to produce systems such as large photonically controlled phased array antennas which conform to an aerodynamic shape or which can be unrolled in space after launch.⁵⁴

Before discussing our work, it is appropriate to note other approaches to flexible organic electro-optic devices. Researchers at Hoechst Celanese some time ago effected lift off using water soluble layers. Fetterman (UCLA) and coworkers used Mylar film as a flexible substrate. Lift off using the poor adhesion of a gold-glass interface was employed by Shi and coworkers at TACAN.

As noted in the earlier sections of this communication, newer electro-optic materials are designed to withstand high processing (e.g., electric field poling) temperatures and thus these require a lift off process that can withstand the higher processing temperatures used with newer materials. The work discussed here is based on an SU-8/Au release interface where SU-8 is a commercial photo-resist that has poor adhesion to a gold surface but good adhesion to a silicon substrate surface. Lift off selected areas are defined by patterning the Au coating on a Si substrate. The multi-step process is illustrated schematically in Fig. 4. The dimensions of a fabricated modulator are given in Fig. 5.

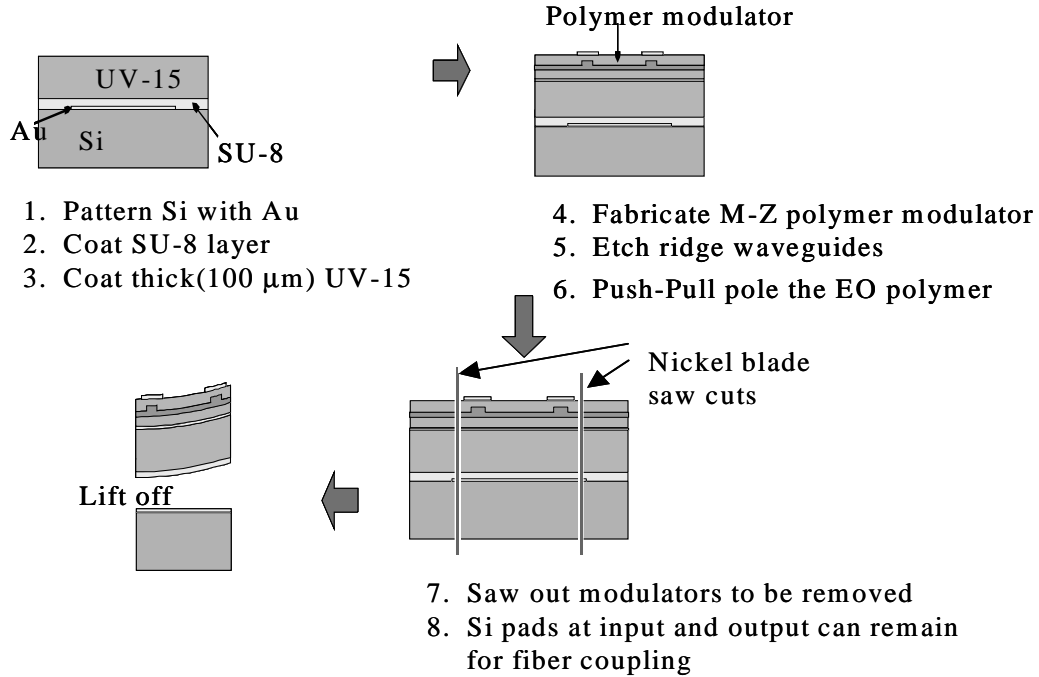


Figure 4. The steps in the fabrication of a flexible modulator are shown.

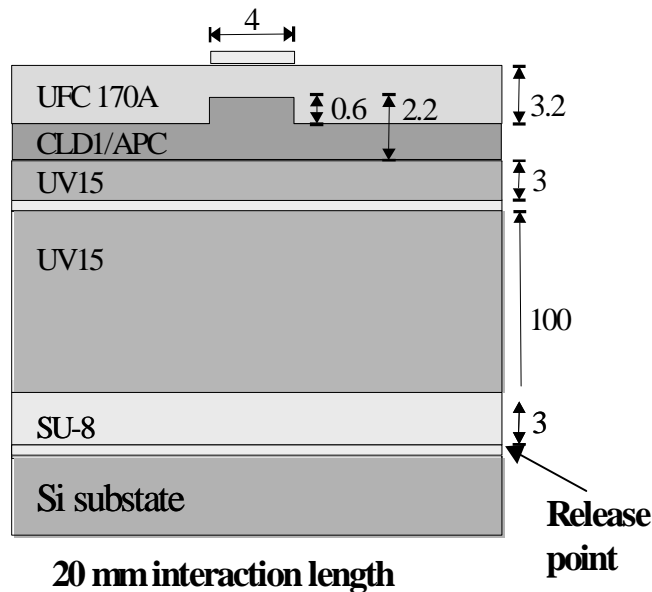


Figure 5. The dimensions (in microns) of the fabricated flexible modulator are shown.

In order to evaluate the performance of polymeric electro-optic modulators with bending and flexing, we have constructed two test beds. The first, adapted for measurement of changes in device parameters with bending, is shown in Fig. 6 while the second (which focuses on measurement of changes with repeated flexing) is shown in Fig. 7.

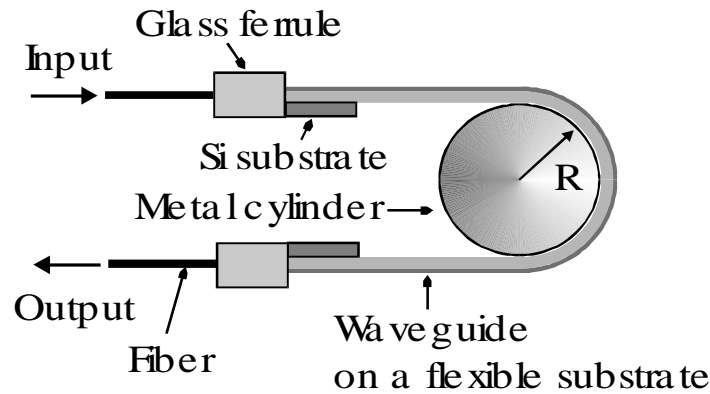


Figure 6. The test arrangement for measurement of changes of device performance with bending is shown

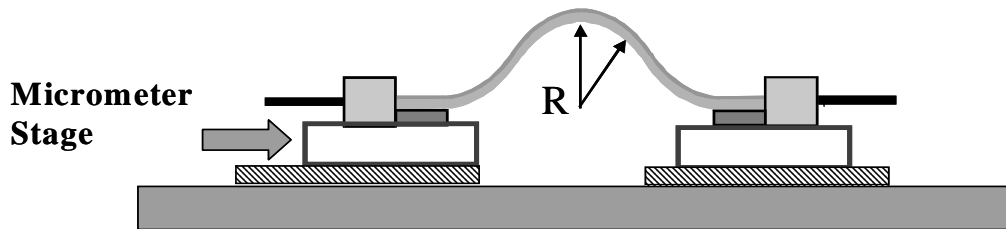


Figure 7. The test bed for measurement of changes in device performance with repeated flexing is shown.

The polymer modulator of Fig. 5 exhibited a V_{π} of 2.6 V at 1.55 microns wavelength and an extinction ratio of greater than 20 dB. This performance is comparable to that organic electro-optic modulators fabricated on rigid substrates. As is evident from a consideration of the following Figs 8-11, no change in waveguide loss is observed with bending radii

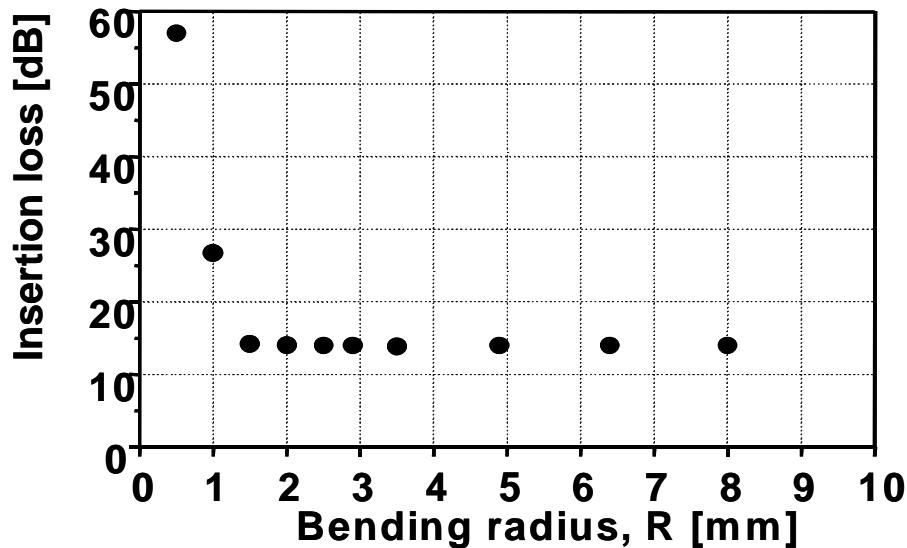


Figure 8. The variation of Insertion Loss (dB) versus bending radius (as defined in Fig. 6) is shown.

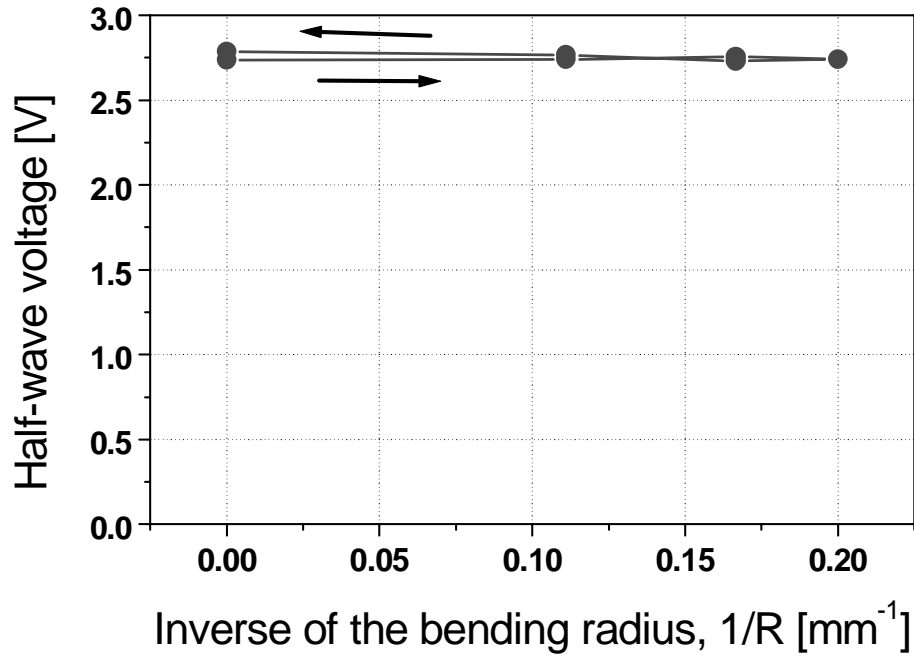


Figure 9. Variation of halfwave voltage with flexing and relaxation (measured using the apparatus of Fig. 7) is shown. The change in V_{π} was less than 2%, which is within experimental error. Note that bending occurs moving toward the right of the figure.

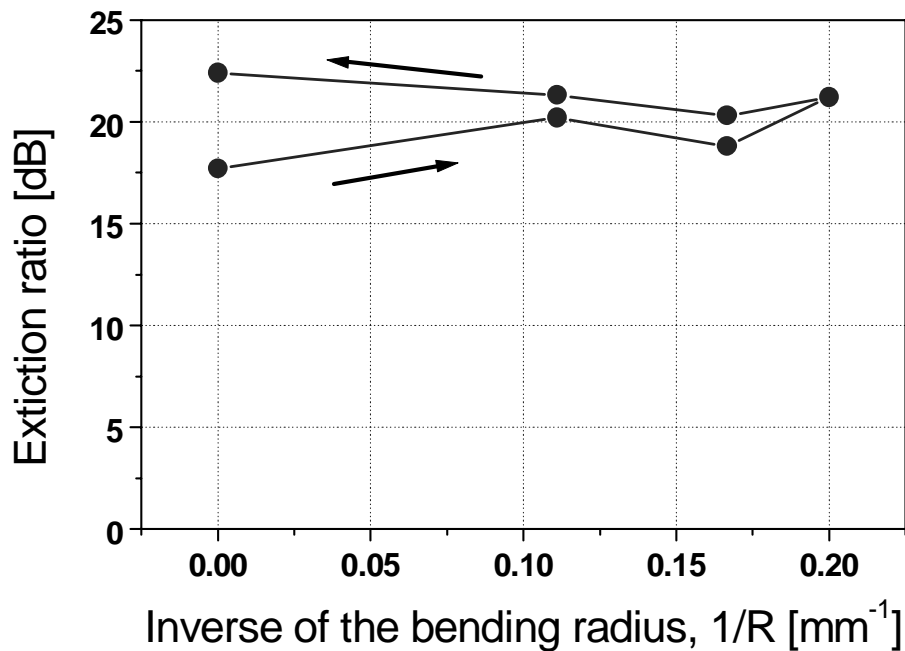


Figure 10. Variation of Extinction Ratio (ER) with flexing and relaxation is shown. The maximum change is about 20% and is likely explained by the strong sensitivity of ER to polarization state.

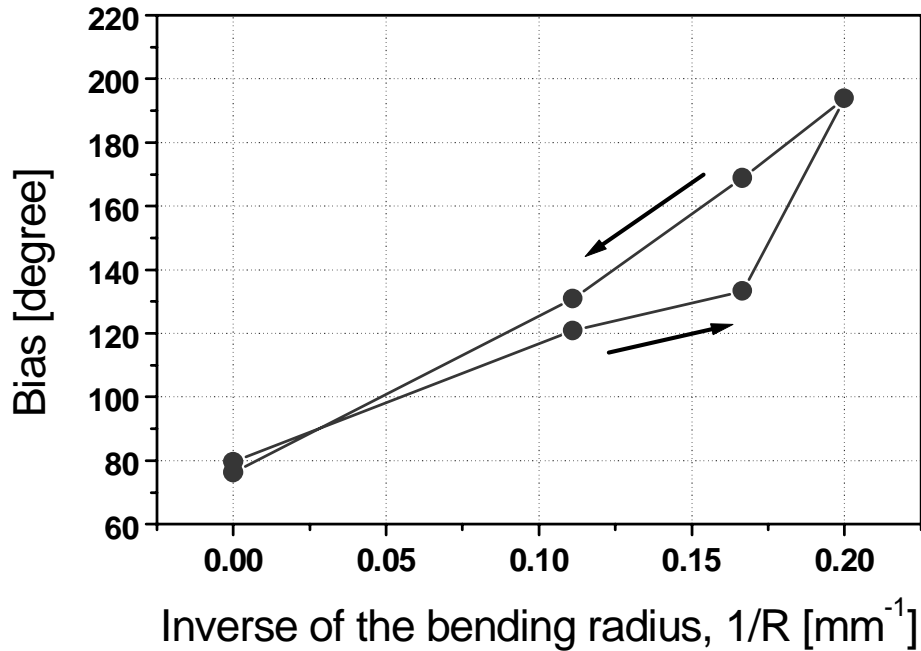


Figure 11. The variation of Bias Point with flexing and relaxation is shown.

until radii of 1.5 mm are reached. No cracking is observed with repeated flexing of the waveguide. No measurable changes in V_π and extinction ratio are observed with repeated flexing and bending to radii of 5 mm. A repeatable shift in modulator bias point is observed as the modulator is flexed (as is evident from Fig. 11). This is believed to be due to strain created in the unbalanced (different optical path lengths) Mach Zehnder modulator.

From the results presented above, it is clear that flexible electro-optic modulators can be fabricated and that for some device structures desired performance can be maintained even under repeated flexing and relaxation.

3.2. Fabrication and characterization of ring microresonators

Ring microresonators afford the opportunity of achieving a long interaction length (and thus reduced V_π) in a very compact (e.g., the size of a human hair or smaller) device structure. They also afford a number of opportunities for special device function such as wavelength selective filtering, active wavelength division multiplexing (WDM), and voltage-controlled wavelength tuning. The use of organic electro-optic materials affords the advantage of relatively easy fabrication of a large number of modulators on a single wafer or chip. Moreover, the ability to achieve three-dimensional integrated circuit structures is an advantage of organic materials that can be put to good use in 3-D reconfigurable optical interconnection. We have recently demonstrated that soft lithography techniques, as well as reactive ion etching techniques, can be used to achieve high-density integration of coupled ring microresonator elements. This advance may permit low cost fabrication of complex ring microresonator architectures. The downsides of using ring microresonator devices structures include increased optical power (and thus the potential for photochemical degradation), reduced bandwidth, and increased optical loss associated with bending and scattering losses, which are more problematic for multiple pass ring microresonators than for single pass stripline devices. The trade off of bandwidth for reduced V_π is not particularly problematic for organic electro-optic materials because bandwidth is typically limited by metal electrodes and the nearly terahertz intrinsic bandwidths of organic electro-optic materials are difficult to realize except in difference frequency generation (e.g., the terahertz signal generation and detection experiments of Hayden). In our first experiments involving single ring microresonators, we demonstrated that a bandwidth of 15 GHz and a bandwidth sensitivity factor of 2GHz/V could be achieved per ring microresonator modulator. Quality (Q) factors on the order of 100,000 are easily obtained with organic electro-optic ring microresonators leading to wavelength selectivity on the order of 0.01 nm at telecommunication wavelengths. Thus, it

is clear that with the fabrication of 50 ring microresonators on a chip that an operational bandwidth of 500 Gb/s could be achieved for active WDM.

Recently, we have explored both all organic ring microresonator structures where both core and cladding materials are organic polymeric materials and organic/silicon structures where silicon represents the core waveguide material and electro-optic organic materials serve as cladding materials. A clear advantage of organic materials is that index of refraction values can be varied widely. The difference between index of refraction of the core and cladding is a critical parameter defining, for example, the radius of the modulator that can be used to achieve acceptable optical loss and free spectral range (FSR) values. In previous publications describing our work on single ring microresonator structures, we have described design considerations and the details of fabricating ring microresonators from polymeric materials.^{23,52} We will not repeat that discussion here but rather will now proceed to describe some of our more recent results on double ring microresonator structures. Before we launch into that discussion it is useful to note that the photostability of organic electro-optic ring microresonator devices is better than we had initially expected and that organic devices have the attractive advantage of permitting fabrication of either athermal (temperature independent) or temperature dependent designs.

In the following discussion, we focus on double ring microresonators. The tuning of a single ring is limited by the Δn that is possible. Increased tuning rate and range can be achieved by using two rings of different diameters in series (a double micro-ring or DMR). The DMR permits exploitation of the Vernier effect shown in Fig. 12.

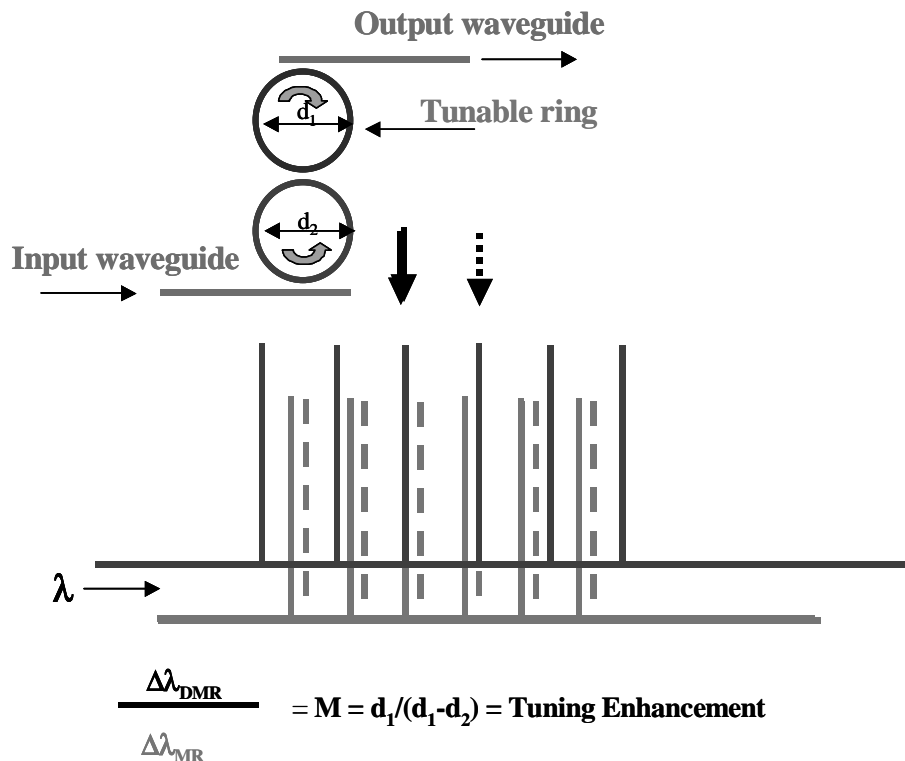


Figure 12. Enhancement of tuning using a double ring resonator is shown. The only way for light to go from the input to the output is to be resonantly coupled into both rings, which is controlled by voltage applied to the electro-optic waveguide material. As voltage is applied different standing modes of the two rings are brought into resonance. The tuning amplification factor, M , relates to difference in the size of the two rings. In the figure, d_1 and d_2 are the diameters of rings 1 and 2 and $\Delta\lambda_{\text{DMR}}$ and $\Delta\lambda_{\text{MR}}$ are the wavelength shifts of the double and single ring microresonators respectively.

In this work we fabricate ring microresonators of 480 and 492 microns leading to an M of 40. The Q factors of the rings are 30,000 and the FSR is 120 GHz. The side mode suppression in our DRMs is greater than 30 dB. A thermal tuning rate of 0.6 nm/mW is observed and a voltage-tuning rate of 0.04 nm/V (10 GHz/V) is observed. With this structure we were able to demonstrate tuning of an oscillator across the band of the erbium amplifier (1520-1560

nm). In our experiments the power out is 1 mW and the tuning speed is limited by the long laser cavity of our source to about 1 microsecond. The structure of our device is shown in Fig. 13 and typical results for electronic electro-optic tuning are shown in Fig. 14.

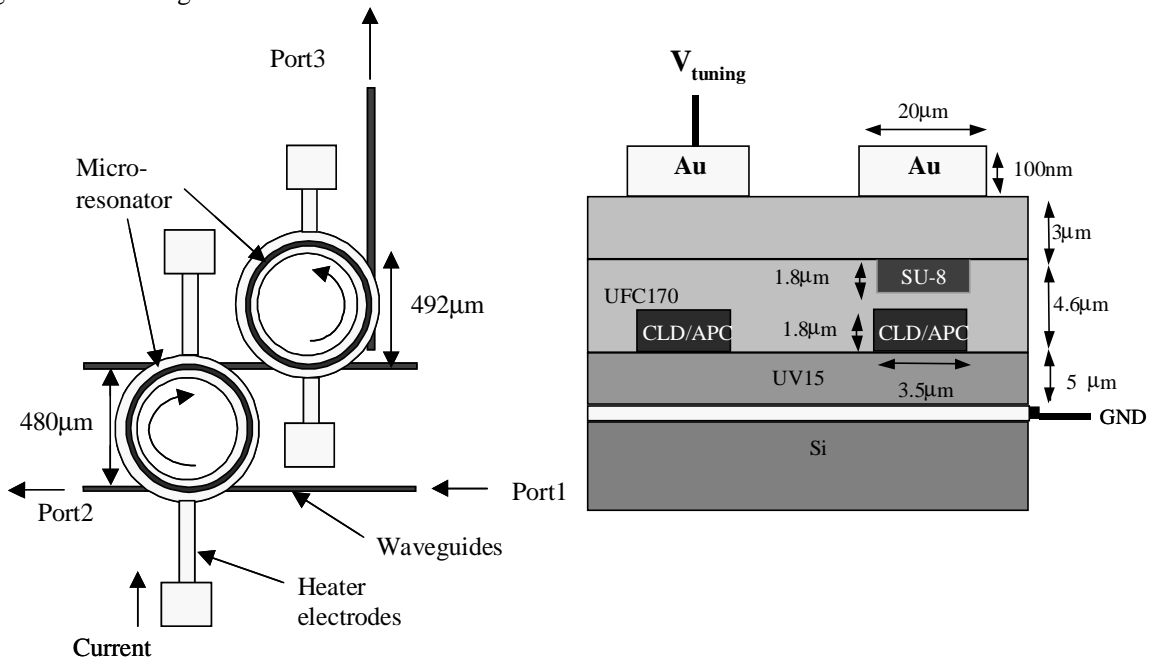


Figure 13. Top and cross-sectional views of our DRM device are shown.

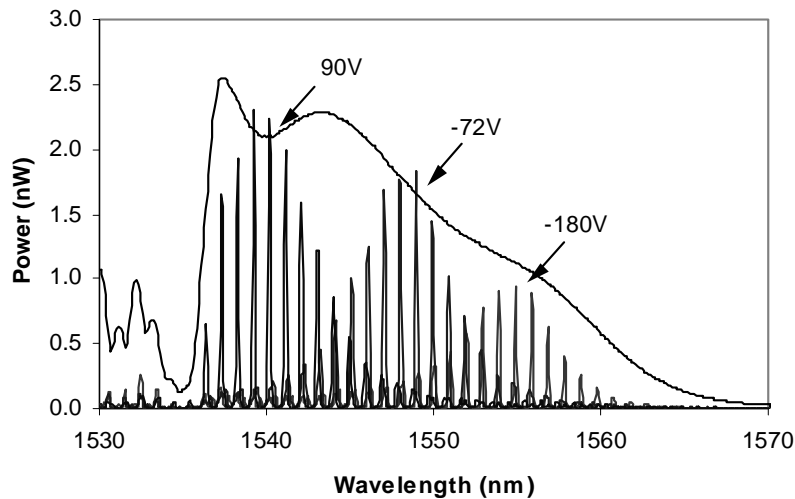


Figure 14. Voltage tuning across the 1.55 micron telecommunications band is shown.

The results reported previously⁵² and shown in this communication were obtained using a CLD/APC composite electro-optic material. Optimum electro-optic coefficients were not achieved in the microresonator structures described.; this deficiency will likely be overcome in time with attention to the details of poling materials for such applications. As noted earlier in this communication, new chromophores represent factors of three improvements over the CLD chromophore in terms of electro-optic activity. Preliminary studies also suggest improved thermal and photostability has been achieved with new chromophores. These new organic electro-optic materials can be expected to lead to improved performance of ring microresonator structures. In addition to the work reported here, we note that Professor

Amnon Yariv (Cal Tech)⁵⁵ has recently fabricated and characterized multi-ring resonator structures, which can be considered a logical extension of the DMR structures discussed here.

4. CONCLUSIONS

Substantial improvements in electro-optic activity have derived and can be anticipated to continue to derive from the theoretical guidance being provided by quantum and statistical mechanical calculations. Electro-optic coefficients on the order of 300 pm/V should become a reality over the next two years. This increase in electro-optic activity should permit enhanced performance to be realized for stripline, prism, and ring microresonator device structures. Operational halfwave voltages of less than one volt should be routinely achieved for a variety of device structures using new materials. For each new material developed for improved electro-optic activity, attention must be given to improving critical auxiliary properties such as optical loss, thermal stability, and photostability. Reasonable design paradigms for control and improvement of these auxiliary properties are now becoming available but more studies need to be made before confidence in meeting the requirements of a broad range of commercial applications is achieved. The dendrimer, dendronized polymer, and supramolecular bundle material that are leading to improved electro-optic activity have the added advantage of permitting rational improvement of auxiliary properties although the exact extent to which photostability can be improved still remains undefined.

The processability and adaptability of organic electro-optic materials is a substantial advantage. Clearly, conformal and flexible device structures are possible and the performance demonstrated in this communication can be improved upon. Organic electro-optic materials are particularly attractive for use in fabricating ring microresonator structures. The dimensions of such devices and other performance properties can be varied significantly by choice of core and cladding materials and the ease of processing of organic materials including by spin casting, vapor deposition, and solution phase deposition provides a unique opportunity for efficient and low cost fabrication. Both thermal and athermal designs can be implemented. The high density of microresonator devices that can be fabricated on a single wafer affords the potential for enormous bandwidth for applications such as active wavelength division multiplexing.

In summary, although organic electro-optic materials have been the subject of investigation for several decades, the next several years are likely to witness dramatic improvements in both material and device performance.

5. ACKNOWLEDGEMENTS

The authors gratefully acknowledge the National Science Foundation and the Air Force Office of Scientific Research for financial support.

REFERENCES

1. D. Chen, H. R. Fetterman, A. Chen, W. H. Steier, L. R. Dalton, W. Wang, and Y. Shi, *Proc. SPIE*, **3006**, 314-317 (1997).
2. D. Chen, H. R. Fetterman, A. Chen, W. H. Steier, L. R. Dalton, W. Wang, and Y. Shi, *Appl. Phys. Lett.*, **70**, 3335-3337 (1997).
3. D. Chen, D. Bhattacharya, A. Udupa, B. Tsap, H. R. Fetterman, A. Chen, S. S. Lee, J. Chen, W. H. Steier, and L. R. Dalton, *IEEE Photon. Tech. Lett.*, **11**, 54-56 (1999).
4. M. Lee, H. E. Katz, C. Erben, D. M. Gill, P. Gopalan, J. D. Heber, and D. J. McGee, *Science*, **289**, 1404-1407 (2002).
5. *Electrical and Optical Polymer Systems: Fundamentals, Methods and Applications*, edited by D. Wise, G. Wnek, D. Trantolo, T. Cooper, J. Gresser, Marcel Dekker, New York, NY, 1998.
6. L. Dalton, A. Harper, A. Ren, F. Wang, G. Todorova, J. Chen, C. Zhang, and M. Lee, *Ind. Eng. Chem. Res.*, **38**, 8-33 (1999).
7. L. R. Dalton in *Advances in Polymer Science, Vol. 158*, edited by K. S. Lee, Springer, Heidelberg, pp. 1-86, 2002.
8. L. R. Dalton, *J. Phys.: Condens. Matter*, **15**, R897-R934 (2003).
9. B. F. Levine and C. G. Bethrea, *J. Chem. Phys.*, **65**, 1989-2682 (1976).
10. D. R. Kanis, M. A. Ratner, and T. J. Marks, *Chem. Rev.*, **94**, 195-242 (1994).
11. S. R. Marder and J. W. Perry, *Science*, **263**, 1706-1707 (1994).
12. S. R. Marder, B. Kippelen, A. K. Y. Jen, and N. Peyghambarian, *Nature*, **388**, 845-851 (1997).

13. E. M. Breitung, C. F. Shu, and R. J. McMahon, *J. Am. Chem. Soc.*, **122**, 1154-1160 (2000).
14. A. Qin, F. Bai, and C. Ye, *J. Mol. Struct. (Theochem)*, **631**, 79-85 (2003).
15. M. C. Ruiz Delgado, V. Hernandez, J. Casado, J. T. Lopez Navarrete, J. M. Raimundo, P. Blanchard, and J. Roncali, *Chem. Eur. J.*, **9**, 3670-3682 (1993).
16. P. A. Sullivan, S. Bhattacharjee, B. E. Eichinger, K. Firestone, B. H. Robinson, and L. R. Dalton, "Exploration of series type multifunctionalized nonlinear optical chromophore concept," *Proc. SPIE*, **5351** (2004).
17. O. V. Prezhdo, *Adv. Mater.*, **14**, 597-600 (2002).
18. L. R. Dalton, A. W. Harper, and B. H. Robinson, *Proc. Natl. Acad. Sci. USA*, **94**, 4842-4847 (1997).
19. B. H. Robinson and L. R. Dalton, *J. Phys. Chem.*, **104**, 4785-4795 (2000).
20. L. R. Dalton, B. H. Robinson, R. Nielsen, A. K. Y. Jen, and W. H. Steier, *Proc. SPIE*, **4798**, 1-10 (2002).
21. L. R. Dalton, B. H. Robinson, A. K. Y. Jen, W. H. Steier, and R. Nielsen, *Opt. Mater.*, **21**, 19-28 (2003).
22. Y. Shi, C. Zhang, H. Zhang, J. H. Bechtel, L. R. Dalton, B. H. Robinson, W. H. Steier, *Science*, **288**, pp. 119-122 (2000).
23. L. Dalton, B. Robinson, R. Nielsen, A. Jen, D. Casmier, P. Rabiei, and W. Steier, *Proc. SPIE*, **4991**, 508-519 (2003).
24. W. K. Kim and L. M. Hayden, *J. Chem. Phys.*, **111**, 5212-5222 (1999).
25. B. H. Robinson, private communication to be published in *J. Phys. Chem.*
26. L. R. Dalton, *Pure and Appl. Chem.*, in press.
27. P. Zhu, M. E. van der Boom, H. Kang, G. Evmenenko, P. Dutta, and T. J. Marks, *Chem. Mater.*, **14**, 4982-4989 (2002).
28. T. J. Marks, S. T. Ho, Z. Liu, P. Zhu, D. G. Sun, J. Ma, Y. Xiao and H. Kang, *Proc. SPIE*, **4991**, 133-143 (2003).
29. J. R. Heflin, C. Figura, D. Marciu, Y. Liu, and R. O. Claus, *Appl. Phys. Lett.*, **74**, 495-497 (1999).
30. J. Luo, S. Liu, M. Haller, H. Li, T. D. Kim, K. S. Kim, H. Z. Tang, S. H. Kang, S. H. Jang, H. Ma, L. R. Dalton, and A. K. Y. Jen *Proc. SPIE*, **4991**, 520-529 (2003).
31. J. Luo, T. D. Kim, H. Ma, S. Liu, S. H. Kang, S. Wong, M. A. Haller, S. H. Jang, H. Li, R. R. Barto, C. W. Frank, L. R. Dalton, and A. K. Y. Jen, *Proc. SPIE*, **5224**, 104-112 (2003).
32. A. K. Jen, J. Ma, T. Sassa, S. Liu, S. Suresh, L. R. Dalton, and M. Haller, *Proc. SPIE*, **4461**, 172-179 (2001).
33. H. Ma, S. Liu, J. Luo, S. Suresh, L. Liu, S. H. Kang, M. Haller, T. Sassa, A. K. Y. Jen, and L. R. Dalton, *Adv. Funct. Mater.*, **12**, 565-574 (2002).
34. H. Ma, A. K. Y. Jen, and L. R. Dalton, *Adv. Mater.*, **14**, 1339-1365 (2002).
35. S. H. Kang, J. Luo, H. Ma, R. R. Barto, C. W. Frank, L. R. Dalton, and A. K. Y. Jen, *Macromolecules*, **36**, 4355-9 (2003).
36. S. Liu, M. A. Haller, H. Ma, L. R. Dalton, S. H. Jang, and A. K. Y. Jen, *Adv. Mater.*, **15**, 603-607 (2003).
37. A. Galvan-Gonzalez, K. D. Belfield, G. I. Stegeman, M. Canva, S. R. Marder, K. Staub, G. Levina, and R. J. Twieg, *J. Appl. Phys.*, **94**, 756-763 (2003).
38. S. M. Garner, S. S. Lee, V. Chuyanov, A. Chen, A. Yacoubian, W. H. Steier, and L. R. Dalton, *IEEE J. of Quantum Electronics*, **35**, 1146-1155 (1999).
39. W. Steier, A. Chen, S. Lee, S. Garner, H. Zhang, V. Chuyanov, L. Dalton, F. Wang, A. Ren, C. Zhang, G. Todorova, A. Harper, H. Fetterman, D. Chen, A. Udupa, D. Bhattacharya, and B. Tsap, *Chem. Phys.*, **245**, 487-506 (1999).
40. A. Chen, V. Chuyanov, F. I. Marti-Carrera, S. M. Garner, W. H. Steier, J. Chen, S. S. Sun, L. R. Dalton, *Opt. Eng.*, **39**, 1507-1516 (2000).
41. S. S. Lee, A. H. Udupa, H. Erlig, H. Zhang, Y. Chang, C. Zhang, D. H. Chang, D. Bhattacharya, B. Tsap, W. H. Steier, L. R. Dalton, and H. R. Fetterman, *IEEE Microwave and Guided Wave Letters*, **9**, 357-359 (1999).
42. C. Zhang, L. R. Dalton, M. C. Oh, H. Zhang, W. H. Steier, *Chem. Mater.*, **13**, 3043-3050 (2001).
43. M. C. Oh, H. Zhang, C. Zhang, H. Erlig, Y. Chang, B. Tsap, D. Chang, A. Szep, W. H. Steier, H. R. Fetterman, L. R. Dalton, *IEEE J. Sel. Top. Quant. Electron.*, **7**, 826-835 (2001).
44. J. H. Bechtel, Y. Shi, H. Zhang, W. H. Steier, C. H. Zhang, and L. R. Dalton, *Proc SPIE*, **4114**, 58-64 (2001).
45. H. R. Fetterman, D. H. Chang, H. Erlig, M. Oh, W. H. Steier, and L. R. Dalton, *Proc. SPIE*, **4114**, 44-57 (2001).
46. H. Zhang, M.-C. Oh, A. Szep, W. H. Steier, C. Zhang, L. R. Dalton, H. Erlig, Y. Chang, D. H. Chang, and H. R. Fetterman, *Appl. Phys. Lett.*, **78**, 3136-3138 (2001).
47. J. Han, B. J. Seo, H. R. Fetterman, H. Zhang, and C. Zhang, *Proc. SPIE*, **4991**, 562-574 (2003).
48. J. H. Bechtel, J. Menders, and D. Y. Zang, *Proc. SPIE*, **4991**, 552-561 (2003).

49. L. Sun, J. H. Kim, C. H. Jang, J. J. Maki, D. An, Q. Zhou, X. Lu, J. M. Taboada, R. T. Chen, S. Tang, H. Zhang, W. H. Steier, A. S. Ren, and L. R. Dalton, *Proc SPIE*, **3950**, 98-107 (2000).
50. J. H. Kim, L. Sun, C. H. Jang, D. An, J. M. Taboada, Q. Zhou, X. Lu, R. T. Chen, B. Li, X. Han, S. Tang, H. Zhang, W. H. Steier, A. S. Ren, and L. R. Dalton, *Proc SPIE*, **4279**, 37-44 (2001).
51. L. Sun, J. Kim, C. Jang, D. An, X. Lu, Q. Zhou, J. M. Taboada, R. T. Chen, J. J. Maki, S. Tang, H. Zhang, W. H. Steier, C. Zhang, and L. R. Dalton, "Polymeric Waveguide Prism Based Electro-Optic Beam Deflector," *Opt. Eng.*, **40**, 1217-1222 (2001).
52. P. Rabiei, W. H. Steier, C. Zhang, and L. R. Dalton, *J. Lightwave Technology*, **20**, 1968-1975 (2002).
53. B. Maune, R. Lawson, C. Gunn, A. Scherer, and L. Dalton, *Appl. Phys. Lett.*, **83**, 4689-4691 (2003).
54. H. C. Song and W. H. Steier, private communication to be published in *Appl. Phys. Lett.*
55. A. Yariv, private communication to be published in *J. Phys. Chem.*